Materials Chemistry and Physics 329 (2025) 130061

Contents lists available at ScienceDirect

Materials Chemistry and Physics

journal homepage: www.elsevier.com/locate/matchemphys

Eco-sustainable and flexible SERS platform based on waste cellulose decorated by Ag nanoparticles

D. Giuffrida [a], D. Spadaro [a,*], V. Strano [b], S. Trusso [a,**], M.L. Saladino [a,c], F. Armetta [a,c], R.C. Ponterio [a]

[a] Istituto per I Processi Chimico-Fisici del Consiglio Nazionale delle Ricerche, V.le F. S. d'Alcontres 37, 98158, Messina, Italy
[b] Istituto per la Microelettronica e Microsistemi del Consiglio Nazionale delle Ricerche, Via S. Sofia 64, 95123, Catania, Italy
[c] Dipartimento Scienze e Tecnologie Biologiche, Chimiche e Farmaceutiche, STEBICEF and INSTM UdR - Palermo, Università di Palermo, Viale delle Scienze pad. 17, Palermo, 90128, Italy

HIGHLIGHTS

- Innovative approach by utilizing recycled cellulose as substrates for SERS sensors.
- Optimization of SERS response through controlled deposition conditions.
- Use of recycled paper through renewable sourcing and eco-friendly production processes.
- Promotion the reuse of waste materials.
- Fabrication process avoids harmful chemicals, utilizing natural drying methods and sustainable production practices.

GRAPHICAL ABSTRACT

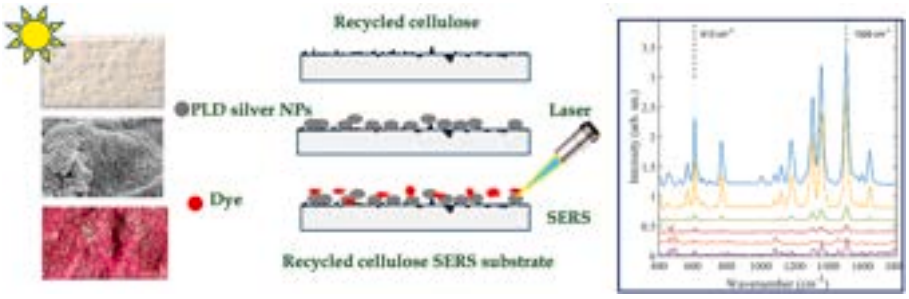

ARTICLE INFO

Keywords:
Recycled paper
SERS sensor
Sustainability
Raman spectroscopy
Flexible devices

ABSTRACT

This paper presents an innovative and environmentally friendly technology for the fabrication of low-cost SERS (Surface-Enhanced Raman Spectroscopy) sensors based on flexible substrates made of cellulose fibers reclaimed from waste. The substrates are decorated with nanostructured silver (Ag) thin films produced by pulsed laser deposition (PLD). In this process, the deposition conditions (laser fluence, gas pressure, target-substrate distance, deposition time, etc.) were optimized to enhance the SERS response. Different types of paper with different textures were tested, as it was also observed that the paper roughness significantly influences SERS efficiency. The samples were characterized using UV–Vis absorption spectroscopy, SEM microscopy, and surface profilometry to evaluate both the paper and the deposited films' morphologies. The SERS activity was assessed by detecting Rhodamine 6G in aqueous solutions drop-casted on the sensors, with concentrations ranging from 10^{-2} M to 10^{-10} M. Measurements were carried out using a handheld instrument equipped with dual excitation laser lines centered at 785 nm and 833 nm. The observed lower detection limit of 10^{-10} M was achieved across all paper types tested. These results demonstrate the potential of integrating smart, eco-friendly materials in the fabrication of chemical sensors for sustainable advancement in environmental monitoring and safety. The materials not only exhibit excellent sensing capabilities but also minimize ecological footprints through renewable

* Corresponding author.
** Corresponding author.
E-mail addresses: donatella.spadaro@cnr.it (D. Spadaro), sebastiano.trusso@cnr.it (S. Trusso).

https://doi.org/10.1016/j.matchemphys.2024.130061
Received 12 August 2024; Received in revised form 9 October 2024; Accepted 15 October 2024
Available online 17 October 2024

sourcing and eco-friendly production processes. While the deposition protocol is well-established for other substrates, this study marks the first exploration of its use on biomass-derived substrates.

1. Introduction

In the last decade, sustainability, reuse and recycle have become essential practices, particularly in physics and chemistry laboratories. In every research sector, in fact, from environment to energy through economy and Cultural Heritage a transition to more environmentally friendly processes and methods is required. In recent years, our planet has been hit by severe and close emergency situations that have forced governments to remodulate their list of priorities. After the COVID-19 pandemic, the European Union (EU) has been at the forefront of promoting sustainable practices, encouraging the use of renewable resources through key initiatives [1,2], which emphasize the importance of transitioning to a more sustainable, resource-efficient and circular economy. In turn, this has spurred renewed interest in eco-friendly, recyclable materials across various research sectors and industry.

The world of research and scientific laboratories represents a significant consumer of raw materials, particularly in the field of material science, most of which eventually become waste after their use. A first step in the direction of a zero-environment impact practice can be made by obtaining raw materials from secondary sources (waste materials). From this point of view, in the last few years, researchers worldwide have developed environmentally friendly materials derived from biopolymers [3], including cellulose [4], to replace plastics [5] or other materials that can play a significant role to carbon dioxide emissions [6]' as a result of their production or use.

Cellulose fibers (primary and secondary) are raw materials with large availability among existing vegetal and renewable resources [7]. Recycled paper can be sourced from various industrial processes, each tailored to its intended application. A specific eco-friendly variant can be produced without chemicals and pollutants, circumventing whitening procedures. This holds particular significance for its integration into devices designed for chemical species detection [8,9].

In Cultural Heritage (CH) sector, the identification of compounds (as dyes, pigments and colorants) and degradation products is a crucial aspect, due to its strong repercussions on historical analysis and conservation perspectives. While numerous analytical methods exist for dye identification, they sometimes can struggle with problematic organic dyes or when analyzing the minute sample sizes typically necessary in the examination of artworks [10–12]. For instances, conventional Raman spectroscopy [13], a valuable non-destructive technique for identifying precise molecular fingerprints, can faces two primary challenges when analyzing several heritage materials for at least two reasons: first, many analytes including natural and synthetic dyes have inherently low Raman scattering cross sections, which limits the signal intensity [14,15]; second, some organic compounds often exhibit fluorescence that obscures the underlying Raman peaks and degrades spectral quality.

From this point of view surface-enhanced Raman Spectroscopy (SERS) can overcome these drawbacks. In SERS the Raman scattering signal of molecules adsorbed on a nanostructured metal surface (gold, silver and other metals) is strongly amplified [16], moreover the interaction with metal structure can lead to the fluorescence quenching improving the signal to noise ratio.

In previous works, substrates such as glass, polishing paper and polymeric film have been tested for the SERS analysis of model dyes like alizarin, purpurin, and indigo, with high efficiency and reproducibility [17,18], [19–22]. However, these substrates have limitations, such as a lack of flexibility and poor eco-compatibility. On the other hand, cellulose offers an ideal supporting substrate for plasmonic SERS sensors compared to rigid platforms [23–25]. The excellent mechanical strength of paper derived from its embedded cellulose fiber network imparts high flexibility to the substrate. The ability to flex and fold SERS sensors fabricated on paper expands possibilities for non-planar on-site analysis and integration onto irregular heritage artifact surfaces. Moreover, the biodegradability and sustainability of cellulose paper fabricated from renewable biomass resources is advantageous from an environmental perspective, aligning well with green chemistry principles [26] and European strategies [1,2].

Moreover, the intrinsic microscale roughness of the natural texture of the cellulose fiber matrix paper provides additional sites for analyte adsorption and localization in electromagnetic hotspots, increasing the Raman signal enhancement [27] and boosting sensitivity without complex nanofabrication. In recent years, many papers have appeared in the literature demonstrating the possibility of using cellulose-based substrates for the fabrication of active SERS devices [28]. Obviously, many differences between one device and another lie in the type of paper and especially in the realization of the metal film on their surface. This last point clearly has the greatest influence on the SERS properties of the device, depending on the type of metal deposited, and on its morphological characteristics. Many methods were explored to realize a metallic film on the paper surface: drop casting of metallic nanoparticles realized by chemical [29] or physical methods [30]; growth of nanoparticles by thermal evaporation [31]; formation of silver film via reduction of Ag^{+} ions after the immersion of the cellulose paper into proper aqueous solutions [32]; inkjet printing [33,34]. Nevertheless, most of the proposed technique leads to uneven surface morphologies

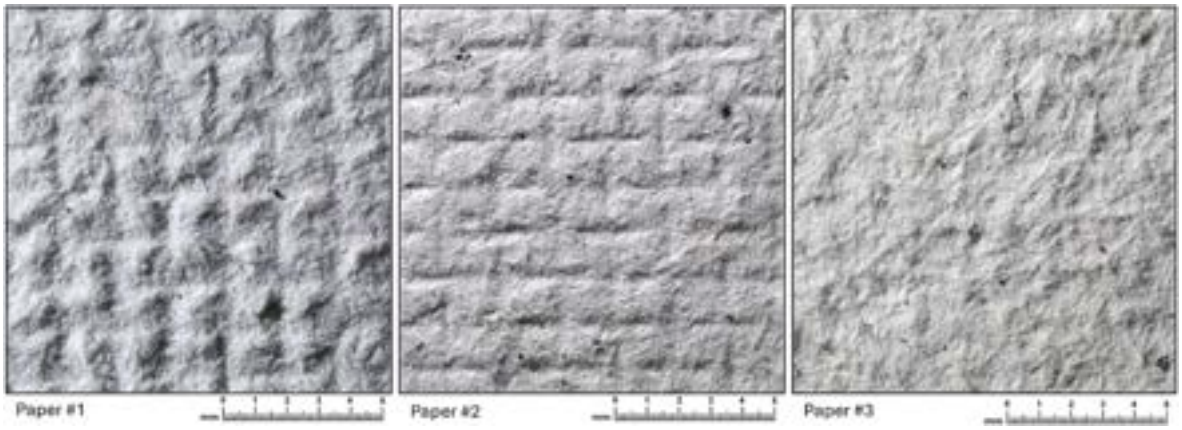

Fig. 1. Textures of the three papers selected as substrates.

with the SERS signal being position dependent, or the use of chemicals and/or thermal treatment.

The current work aims to present an innovative approach to transform paper waste into a valuable resource. Specifically, we employ a single-step decoration method able to produce the complete coverage of the paper substrates with a homogeneous metallic film without the needs of unwanted chemicals or thermal treatment. The fabrication protocol, in fact, involves the use of Pulsed Laser Deposition (PLD) in controlled Argon atmosphere at room temperature for creating nanostructured films with tailored properties coating on the SERS platforms [35].

Once the SERS sensors have fulfilled their primary function, they can be reintroduced into the material cycle where they are processed and transformed into new substrate materials.

The described approach provides a non-invasive 'sampler' entirely based on ecological platform working as a user-friendly, cost-effective, and ready-to-use sensor capable of capturing single grains of the material for analysis. These sustainable sensors are suitable for non-invasive detection and diagnostics in Cultural Heritage materials, but their applications extend beyond this field.

2. Experimental section

Materials. Recycled cellulose substrates from wastepaper were produced by an artisanal and sustainable procedure in order to exclude unwanted chemicals in the final product, paper drying was performed without the use of artificial heat sources (Angolo del CARTigianato - Reggio Calabria Italy). Ag nanoparticles produced by PLD starting from silver target 99.99 %, dia. 15 mm, thick 1 mm from Nanovision srl and Rhodamine 6G from Sigma Aldrich solution used as molecule test.

Selection of paper substrates and preparation of probe molecule solutions. Three types of cellulose substrates handcrafted with slightly different features as texture and morphology were selected from recycled paper obtained from wastepaper streams (Fig. 1), emphasizing sustainability and the reutilization of materials. This selection was carefully made through visual inspection to ensure a different representation of physical characteristics that could influence the SERS performance [36, 37].

The reason behind choosing different substrates was twofold and due to their surface morphology, matrix texture and cellulose fiber density. A paper sample is given by a network of cellulose fibers whose density, size, and their interconnection modality can give rise to very different paper textures. So that, a different behavior of the selected paper samples could be expected even if the Ag films are grown under identical deposition conditions. A rougher surface can provide a larger surface available to the Ag film and hence more "hot spots" – areas where the electromagnetic field is significantly amplified, thus potentially enhancing the SERS effect. Furthermore, the arrangement and the morphology of the fibers in the paper can influence how nanoparticles adhere to the surface and spatially distribute across it. A more irregular fiber matrix might facilitate better entrapment and distribution of nanoparticles, leading to a more uniform and effective SERS substrate. Conversely, a smoother matrix might result in less effective nanoparticle adhesion and distribution, potentially reducing the efficiency substrates. Rhodamine 6G (R6G) was selected as test molecules to evaluate the performance of the cellulose-based SERS substrates and lower detection limits of the sensors.

A progressive dilution was prepared to yield R6G solutions with five concentrations 10^{-2} M, 10^{-4} M, 10^{-6} M, 10^{-8} M to 10^{-10} M. These solutions were drop-casted onto the SERS substrates and plain papers (with no deposition) and left to dry under ambient conditions.

Fabrication of Ag/recycled cellulose based sensor. PLD has been utilized to produce quasi-two-dimensional arrays of Ag NPs on paper substrates [38]. This process generates a plasma plume from the vaporized material that expands perpendicularly from the target material's surface. As a result, material growth occurs on the substrate surface, which, in our application, are paper sheets. The growth mechanism of nanostructured silver thin films was studied in previous papers [39–41].

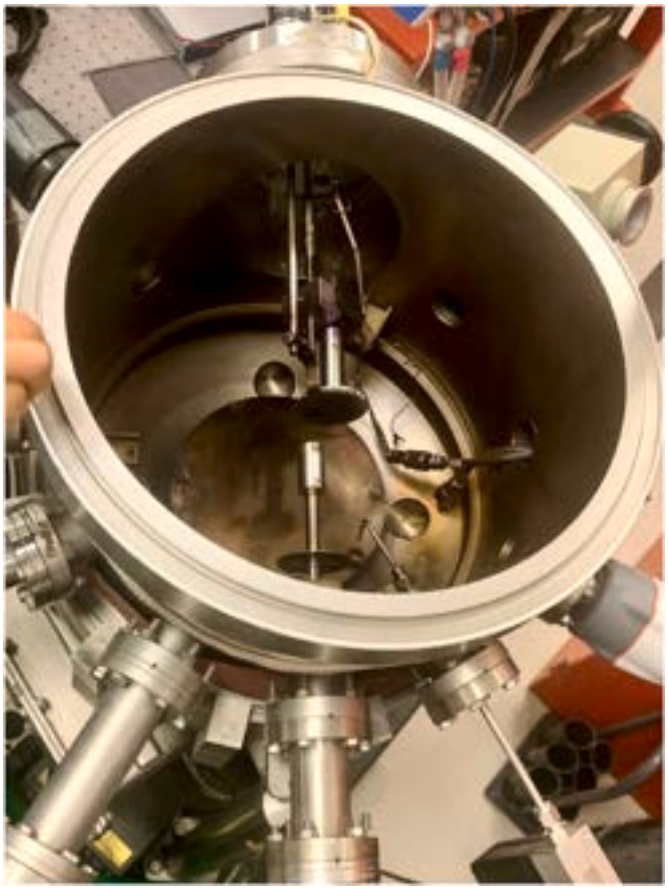

Fig. 2. PLD camera with a recycled paper substrate placed on the rotating holder.

In this process, the NP size is determined by a delicate balance between several parameters: laser fluence, target-to-substrate distance, ambient gas type and pressure, and the ablated mass per pulse. These parameters significantly affect the film's optical, morphological, and structural properties. Key factors influencing SERS activity include the type of metal used, nanostructure size/shape/coverage, excitation wavelength, and adsorbed molecule. Matching the excitation wavelength to the localized surface plasmon resonance of the nanostructures is optimal [42], [43,44].

Controlling the surface morphology is crucial for optimizing the SERS enhancement properties of nanostructured noble metal thin films. In previous studies, we demonstrated that nanostructured Au and Ag thin films can be grown using pulsed laser deposition (PLD) when the ablation process is carried out in a high-pressure inert gas atmosphere. We found that the surface morphology of the films can be controlled by adjusting specific PLD deposition parameters [39], [45, 46]. The greatest SERS enhancement for Ag and Au thin films deposited onto c-Si and glass substrates was achieved when the film surface displayed a complex network of semi-percolated, self-assembled metal islands, resulting from the coalescence of nanoparticles (NPs) generated in the plasma, as consequence of the collisional processes between the ablated atoms and the gas ones. That morphology, in fact, maximizes the density of nanometer-sized gaps between adjacent islands, where localized hot-spots are formed [47]. It was observed that by performing the ablation process in a controlled Ar atmosphere, the surface morphology of the growing film could be adjusted by varying the Ar pressure and the number of laser pulses, while maintaining constant other key deposition

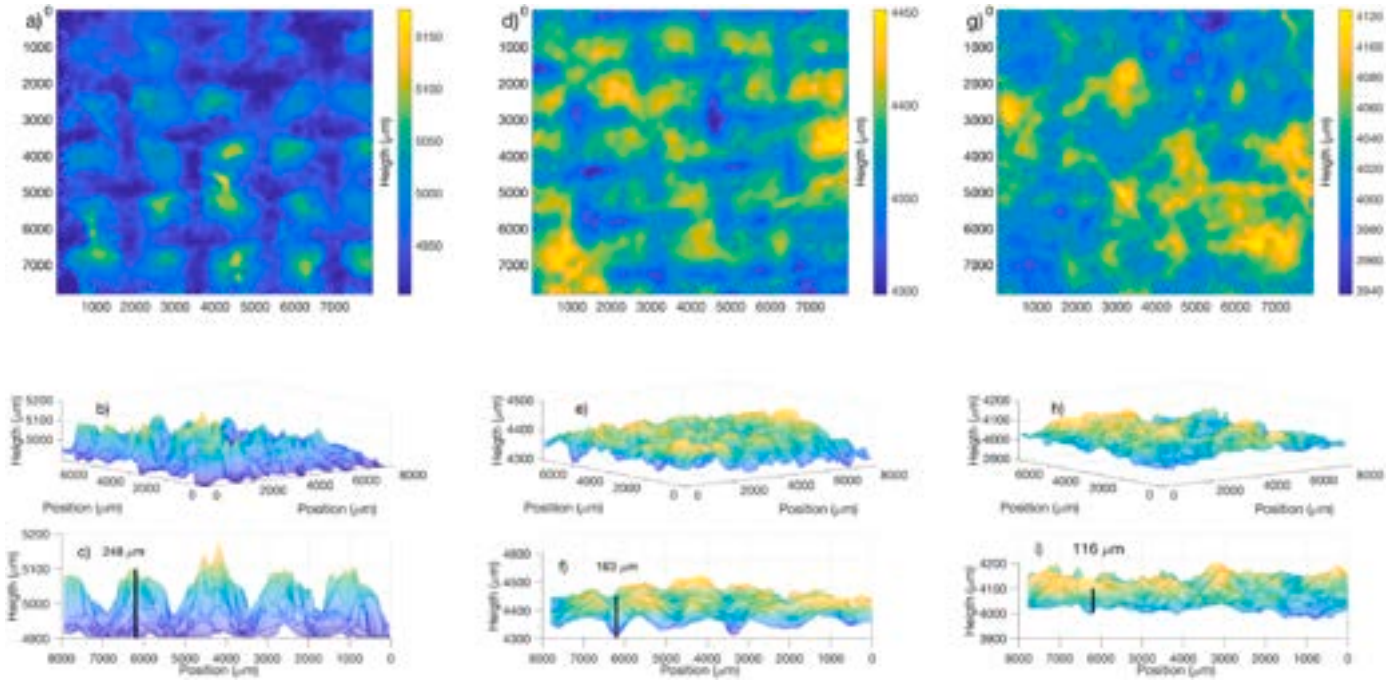

Fig. 3. Laser micro-profilometry maps of the paper samples texture: a) paper #1; b) paper #2; c) paper#3; below are shown the corresponding 3D evidencing the height fluctuations due to the different embossed grids pattern.

parameters such as fluence and target-to-substrate distance. The experimental parameters used in this work were selected to replicate, as closely as possible, the surface morphology that optimized the SERS activity of the silver films deposited on the paper substrates. Films were deposited in a vacuum chamber with a residual pressure lower than 10^{-4} Pa. The target ablation was executed using the third harmonic of a Nd:YAG laser (wavelength 255 nm, pulse width 4 ns, repetition rate 10 Hz) focused with an incidence angle of 45° onto the surface of a silver target (99.95 % purity). The laser spot area, measured using an optical microscope, was approximately 0.37 mm^2, and with a pulse energy of 10 mJ, the resulting fluence was around 2.7 J/cm^2. The target was mounted on a rotating holder to prevent excessive surface damage that might affect the ablation process (e.g. craterization phenomena). Paper substrates, together with glass and c-Si slides, were positioned at 35 mm from the target on a rotating substrate holder. Rotating the substrates enables the deposition of thin films over large areas, around 20 cm^2, ensuring uniform morphology and consistent SERS activity [48]. In order to induce the formation of AgNPs, the deposition process was performed, following our well-established protocol, maintaining the Ar pressure inside the chamber at 70 Pa by a programmable mass flow controller. Furthermore, a c-Si substrate and a glass substrate were additionally placed on the sample holder with the aim to monitoring respectively the morphology (SEM microscopy) of the deposited films and to track the position of the surface plasmon resonance peak (UV–Vis absorption measurements).

Fig. 2 shows the PLD camera with a recycled paper substrate mounted on the rotating holder before the deposition process. To guarantee the homogeneity of the deposition on the surface of the paper sheets, they were fixed to the substrate holder using a set of stainless-steel masks properly designed and built at IPCF mechanical workshop.

Macro-photography, laser and contact micro-profilometry. Macro-photography was employed to acquire high-resolution images of the paper's textures. A Canon M3 camera equipped with a 70 mm-F/2.8 MACRO lens was used coupled with a tripod to ensure stability. Micro-profilometry was used to examine surface morphology and roughness, as these features are crucial for enhancing the Raman signal along with deposition conditions and nanoparticle size and distribution. Indeed, excessively high roughness can reduce nanoparticle uniformity during deposition. The profilometry data allows optimizing paper selection for balance between high sensitivity and reproducible SERS enhancement.

For these purposes, we utilized the laser micro-profilometer *Mini-ConoScan* 3000 by *Optimet Metrology, Ltd.* [49] The instrument, equipped with a patented ConoProbe non-contact sensor, is a compact system designed for high-accuracy 3D scanning, ideal for reverse engineering, quality control, and general 3D applications. It employs conoscopic holography to enable dynamic measurement up to 500 points per second and to collect a set of *x-y-z* spatial coordinates. The variations in surface height are recorded to generate a quantitative topographical map.

The scanning setup consists of a high-precision motorized linear stage (0.1 µm) that can move horizontally on the x and y axes (on which the sample is fixed), a red laser (He–Ne), and a lens with a focal length of 50 mm. When the laser beam emitted by the head strikes the sample, it is reflected and detected by a sensor to determine the distance (with a precision of ±10 µm). After focusing the laser through the lens, a lateral resolution of 16 µm is achieved without loss of detail. Acquisition on paper samples were conducted under the following acquisition parameters: scan mode set to Pulse, power at 12 with Fine Power at 0, and a scanning frequency of 500 Hz.

The field of view covered dimensions of 7.9 mm by 7.9 mm. Data acquisition was resolved into 256 along both the X and Y axes, respectively, yielding resolutions of approximately 30 µm (X) and 30 µm (Y). This was helpful in obtaining an image composed of square pixels, which is crucial for ensuring uniform resolution across the entire image. The measurement was repeated three times, and the average value of the data collected for each pixel was calculated: this calculation is automatically run by the software. The resulting profilometric data were processed using MATLAB@ software.

UV-VIS absorption spectroscopy. Uv–Vis measurements were performed on the samples deposited on Corning glass substrates, spectra were acquired with a home-made UV–vis spectrometer (Avantes AvaLight-DHS Deuterium-Halogen Light Source, Avaspec 2048L spectrometer) in the range 250–1100 nm.

SEM: morphology, size, distribution of AgNPS. The morphology and nanostructure of the cellulose paper mock-up samples before and

after deposition of Ag nanoparticles were investigated by field emission scanning electron microscopy (*FE-SEM, Zeiss Supra 25 instrument*).

The acceleration voltage was varied in the range of 2–3 kV and the analyses were performed using Everhart–Thornley and in-lens detectors. Images were typically resolved at 500–150,000× magnification with an aperture of 30 mm.

SERS analysis. Raman spectroscopy has been employed to acquire Raman spectra on the prepared samples having progressive concentrations to evaluate SERS activity and detection limits. Moreover, it was also used for quality check in the paper deposited with Ag nanostructures, to ensure that no contributions from cellulose were visible after deposition process.

Measurements were conducted using the portable Bruker BRAVO™ handheld Raman spectrometer. The instrument uses two distinct excitation lasers centered at 785 nm and 852 nm in wavelengths. These lasers operate *in tandem* without the possibility to separate their individual contributions at a maximum output of 100 mW and a spot size of ~1 mm^2. One distinctive feature of the dual-laser system is the patented Sequentially Shifted Excitation™ (SSE), a technique designed to reduce the impact of sample fluorescence on the resulting spectra. This dual-laser system provides exceptional sensitivity across a broad spectral range of 300–3200 cm^{-1} with a resolution of 10–12 cm^{-1}, ensuring highly reliable material verification, with a Raman shift accuracy typically better than 1 cm^{-1} in the fingerprint region.

The spectrometer was utilized connected to a dedicated PC running Bruker OPUS software, which allowed for setting acquisition parameters (not available using the handheld unit) and visualizing the results of each measurement.

Multiple point measurements (5) were collected to assess signal uniformity using two integration times: 60 ms (for higher concentrations) and 1200 ms (for the lowest ones).

3. Results and discussion

Macro-photography and Micro profilometry characterization highlighted the morphological features of the substrates analyzed named paper#1, #2, #3.

Fig. 3a–c show different cellulose fiber texture detailed below:

- **paper #1** is characterized by a pronounced fibrous texture with a uniform, tactile surface indicative of its eco-friendly composition. The varied thickness and colors are visible, with occasional dark specks hinting at its previous life. Some darker spots and inconsistencies in the fiber distribution are noticeable. A distinctive feature is the embossed grid pattern, likely imprinted during the drying process, giving the paper a three-dimensional aspect and a raw, natural charm. The profile in Fig. 3b) and c) highlight variations in the Z dimension due to the embossed grid pattern as high as 248 μm.
- **paper #2** is a textured, recycled sample with a less pronounced grid pattern etched into its surface, providing a distinctive tactile experience. It presents a varied fiber composition, with an uneven distribution of color and material due to the environmental production process. The grid lines are more regular compared to the first sample. The rough, organic feel is emphasized by the raised grid, and the matte finish accentuates the natural aesthetics. The 3D plots in Fig. 3d) and f) reveals changes in the surface height of the order of about 163 μm.
- **paper #3** is characterized by a rough, textured surface, interlaced with a complex web of fibers that provide a distinctly organic feel. Unlike the first, this sheet lacks a visible grid pattern, instead presenting a more random, less structured array of fibers. The paper's overall color is a homogenous light gray, punctuated by tiny flecks and specks of darker material, remnants of its recycled origins. The edges of the paper are somewhat frayed, further accentuating its handcrafted quality. The profiles in Fig. 3h) and i) gentle slopes and smaller height changes with respect to the other samples, indicating a smoother surface topography.

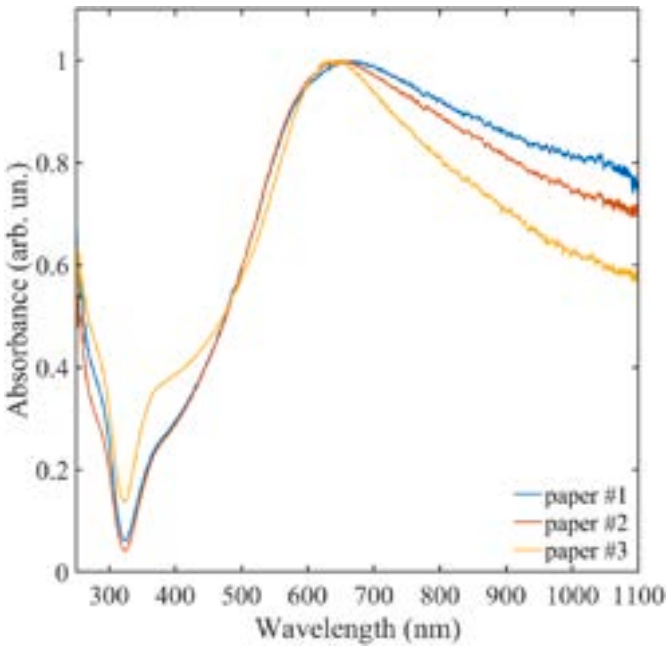

Fig. 4. UV–Vis spectra acquired onto glass substrates covered by Ag NPs in the same deposition processes of the paper substrates

Comparison to SEM data helped relate the synthesized nanostructure to the optical properties.

The UV–Vis spectra shown in Fig. 4 refers to the samples deposited onto glass slide positioned beside the paper sheets. The spectra are normalized to the maximum of the LSPR absorption peak whose shape and position evidence that the Ag films were grown under identical condition for each of the paper sheets used as substrates. They are characterized by the presence of a broad absorption band centered at about 750 nm and extending between 300 and 1100 nm.

In Fig. 5a the morphology of the Ag thin film deposited on the surface of a c-Si substrate with 30000 laser pulses in the presence of an Ar atmosphere of 70 Pa is shown. The morphology is characterized by the presence of islands with complex shapes and smooth edges, separated by a network of inter-connected channels that give raise to a semi-percolated thin film. In Fig. 5b we report the profile extracted along a line of the sample surface, as shown in the inset on the left where the corresponding SEM image is reported. From the profile the morphological features reported above are evident: the islands edges, corresponding to the features with dimension of about 80 nm, the channels corresponding to the deep valley in the profile and the presence of nanoparticles with dimension of about 20 nm. Such a morphology is at the origin of the observed features in the UV–Vis spectra. It is well known, in fact, that the plasmon resonance peak position depends on several factors like nanoparticle size, shape, dielectric environment, and interparticle interactions [50,51], [42,43]. The observed morphology of an array of assembled particles, thus strongly electronically coupled, leads to the broadening of the plasmon resonance peak and its shift to lower energies.

Concerning the growth of the films on the selected paper substrates a different behavior could be expected owing to the very different surface properties of the cellulose fibers with respect to the glass and c-Si surface.

In the images at the lower magnification factor (Fig. 6a–d and g) the different textures of the paper substrates is evident. Paper#1 show a low-density network of cellulose fibers that do not to build up a compact surface as evidenced by the presence of quite large empty areas. On the

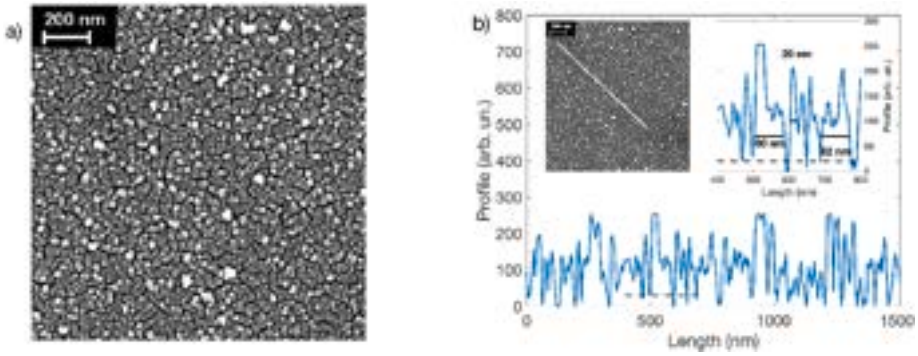

Fig. 5. a: SEM image of the surface of the film deposited onto a c-Si substrate; 5b: Profile of the surface extracted along the line shown in the inset on the left, in the inset on the right a portion of the profile highlighting the observed surface features.

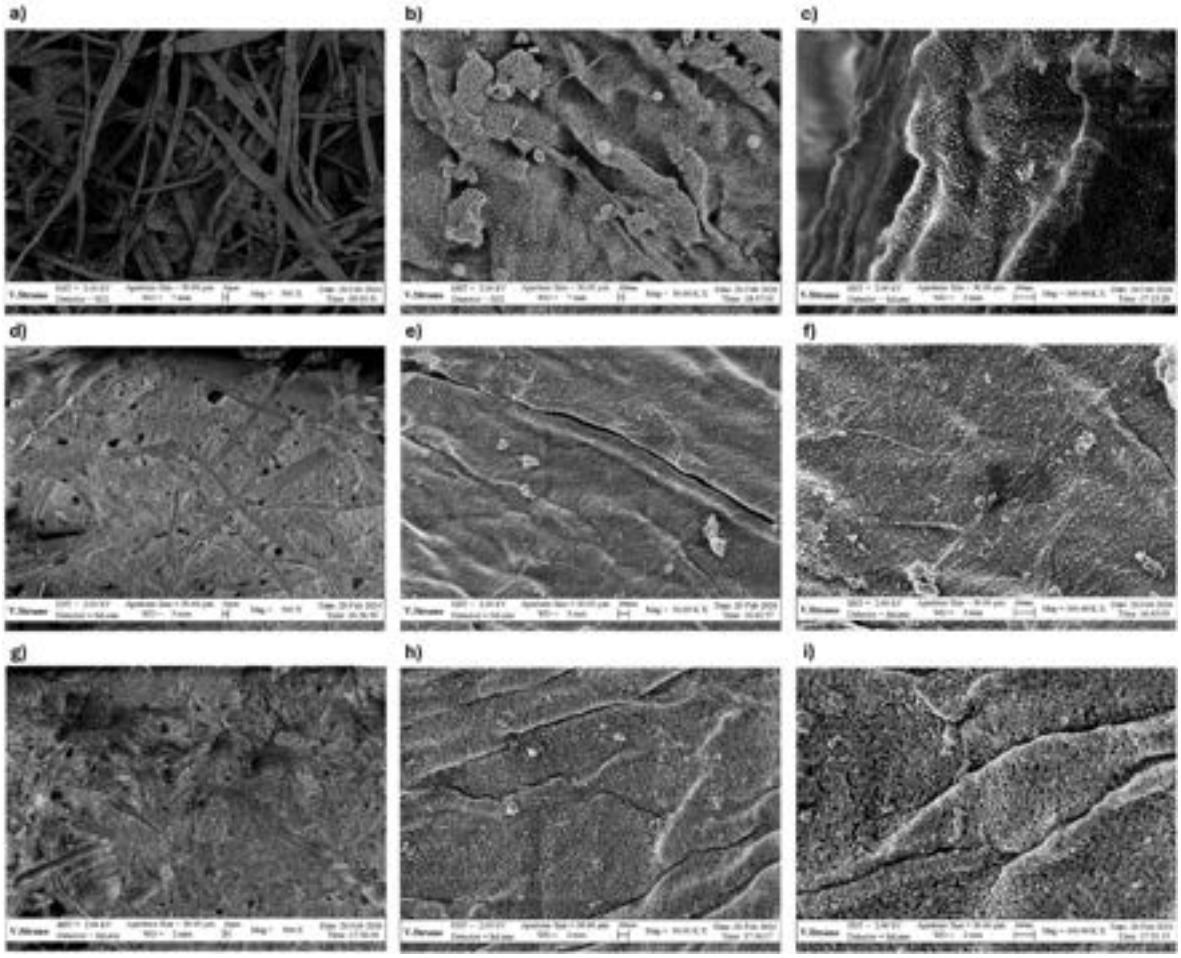

Fig. 6. SEM micrographs, at different magnification factors, of the recycled paper surfaces after the deposition of the silver thin film. a)-c) paper#1; d-f) paper#2; h)-i) paper#3.

contrary paper#2 and paper#3 show a compact surface build up by a network of compressed cellulose fibers, whose presence is still clearly observable. In the images taken at higher magnification factor further details, at the micron or sub-micron level, can be observed. Concerning paper#1 a corrugated and uneven surface is evident, paper#2 and paper3 show a more uniform surface, although some unevenness such as small cracks and reliefs are clearly visible. What is quite remarkable is that the surface of the cellulose fibers, regardless of the underlying structure, results completely covered by the Ag film. This is of paramount importance as far as the SERS activity of the substrates is considered. This result derives from the peculiar features of the PLD technique. As reported in previous works [37] the growth of noble metal thin films deposited by PLD in presence of an inert gas atmosphere proceeds as follows: in a first step the interaction of the laser generated plasma with the ambient gas favors the formation *in flight* of clusters and of nanometric particles. In a second step such nanoparticles land on the substrates with very low residual kinetic energies and start a coalescence process that gives rise to the formation of islands, within such islands the presence of the forming nanoparticles is still observable as it was observed on the surface of the sample deposited on the c-Si. (See

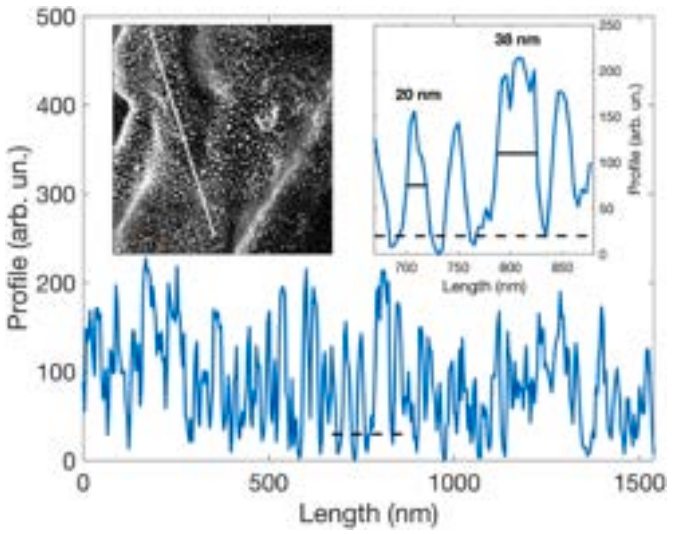

Fig. 7. Profile of the surface of the silver film deposited on paper#1sample, extracted along the line shown in the inset on the left, in the inset on the right a portion of the profile highlighting the observed surface features.

Fig. 5a). Besides the nanoparticles a contribution to the film formation is given by an atomic flux. This atomic component arrives on the substrates and diffuses on the surface aggregating with the structures created by coalesced nanoparticles. In the case of the cellulose fibers the first two steps, *in flight* nanoparticles growth and their coalescence on the substrates are still active, irrespective of the physical properties of the cellulose surface, while the third being strongly dependent on the interaction of the Ag atoms with the cellulose is inhibited. Nevertheless, the resulting morphology of the films on the cellulose substrates is mainly controlled by the first two steps reported above. In order to elucidate this point, we report in Fig. 7 the surface profile extracted from the SEM image of the sample paper#1.

As it can be seen the profile is slightly different the one observed for the sample deposited on the c-Si substrate. The presence of large structures is no more evident while the profile evidences the presence of a continuous assembly of nearly spherical nanoparticles having typical dimension of about 20 nm and separated by spaces having similar lengths, slightly larger structures like the one highlighted in the inset (38 nm) are likely touching nanoparticles. As a consequence, the SERS activity of such substrates should be similar of the one observed for glass or c-Si substrates despite the slightly differences in the surface morphologies.

The SERS intensities were analyzed at the prominent R6G Raman peaks as a function of R6G concentration. This enabled construction of

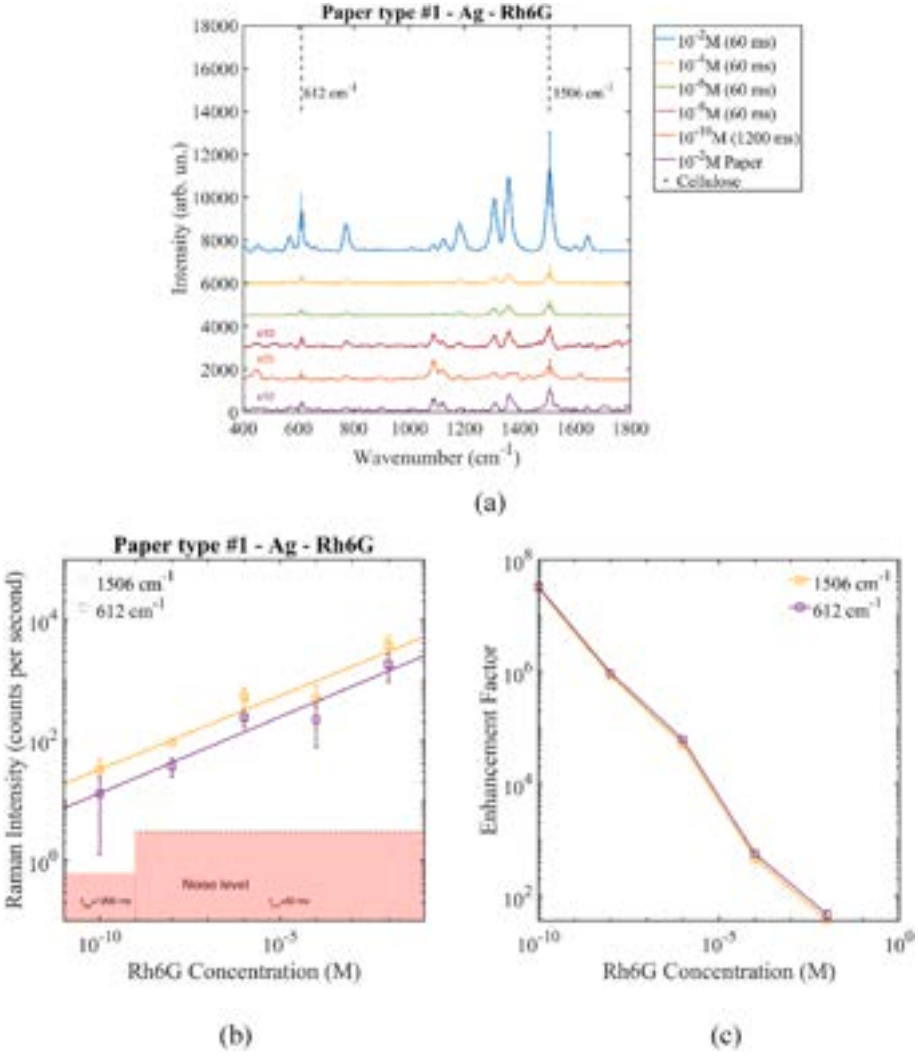

Fig. 8. paper#1: a) SERS spectra of R6G, drop-casted on sensors at concentrations ranging from 10^{-2} M to 10^{-10} M SERS; b) Raman intensity of the R6G characteristic peaks, centered at 1506 and 612 cm^{-1}; c) enhancement factor.

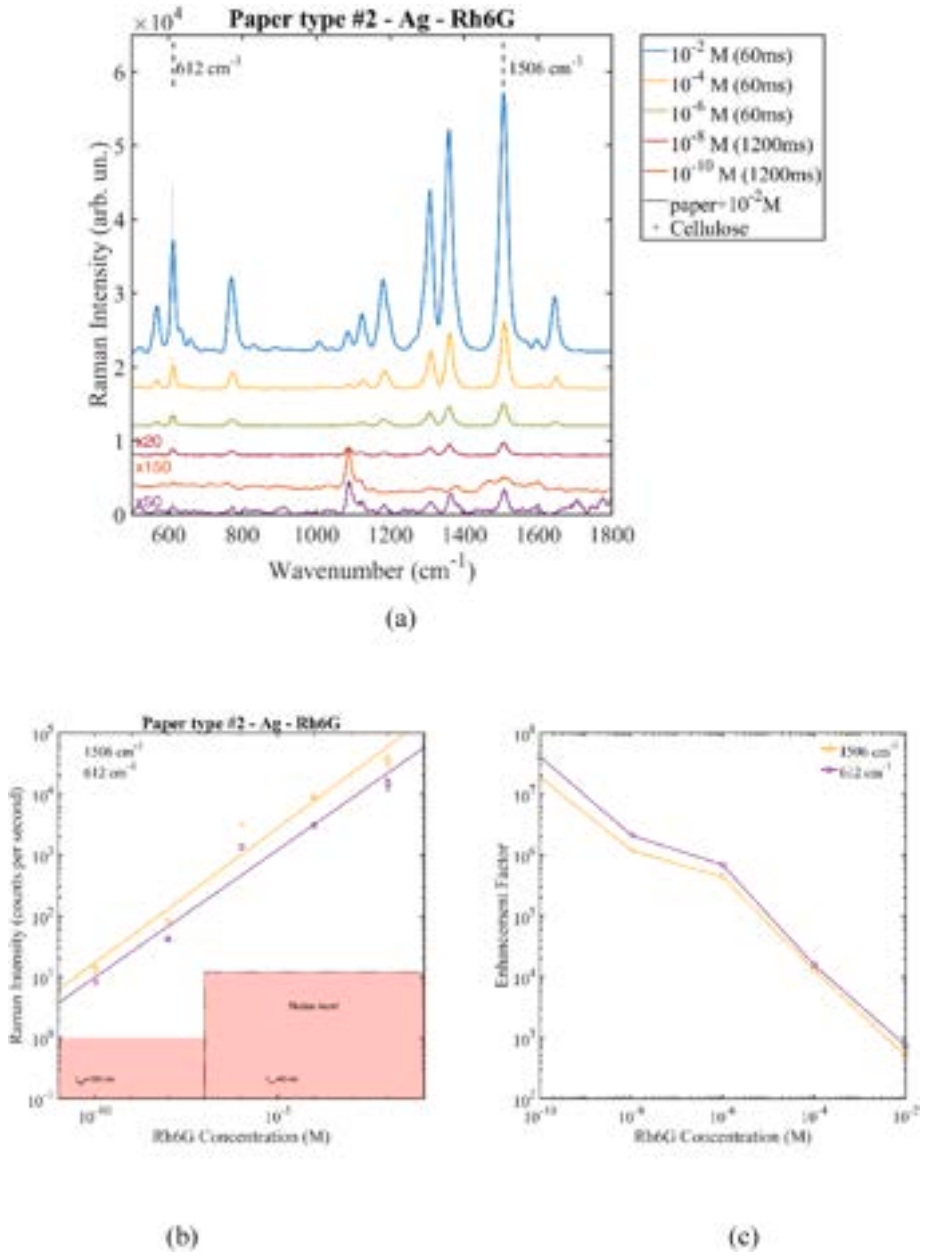

Fig. 9. paper#2: a) SERS spectra of R6G, drop-casted on sensors at concentrations ranging from 10^{-2} M to 10^{-10} M SERS; b) Raman intensity of the R6G characteristic peaks, centered at 1506 and 612 cm^{-1}; c) enhancement factor.

calibration curves and estimation of lower detection limits for each paper type. The acquired datasets provided critical insights into the relationship between surface nanostructure, uniformity, analyte adsorption and SERS enhancement for the recycled cellulose substrates.

On paper#1 (Fig. 8a), SERS spectra acquired across a wide range of R6G concentrations from 10^{-2} M to 10^{-10} M showed clear Raman peaks even at the lowest concentration of 10^{-10} M. The intensity of Raman peaks at 612 cm^{-1} C–C–C ring in plane bending, and 1506 cm^{-1} C–C aromatic stretching [52] decreases as the concentration of Rh6G decreases (Fig. 8b). The error bars indicate the standard deviation of the two peaks intensities across five spectra obtained at different spots on the samples surface. Calibration curves for the same peaks exhibited a linear relationship between peak intensity and R6G concentration on a log-log scale. The noise level, expressed as the standard deviation of the observed noise in a portion of the spectrum free from Raman signatures, is indicated for two integration times, 60 ms and 1200 ms, a longer integration time, in fact, was needed to achieve a good signal to noise ratio for the detection of Rh6G peaks at the lowest concentration level of 10^{-10} M.

The 8c figure illustrates the enhancement factor (EF), which is the ratio of the intensities between the SERS signal and the conventional Raman signal (IRaman) EF=(SERS/NSERS)/(IRaman/NRaman), normalized by the respective analyte concentrations. NSERS and NRaman indicates the number of molecules contributing to the SERS and normal Raman intensities, respectively. There is a noticeable decrease in EF with increasing Rh6G concentration, indicating that the SERS effect is more pronounced at lower dye concentrations. The observation that the EF is not constant and is higher at lower Rh6G concentrations may suggest a distribution of hot spot sites with varying enhancement factors on the substrate. This non-uniformity is a subject of ongoing investigation and could point to the physical characteristics of the SERS substrate or the aggregation state of the nanoparticles used for enhancement [53].

For Paper #2 (Fig. 9), the spectra acquired with the same R6G concentrations demonstrate a decrease in intensity for the Raman peaks

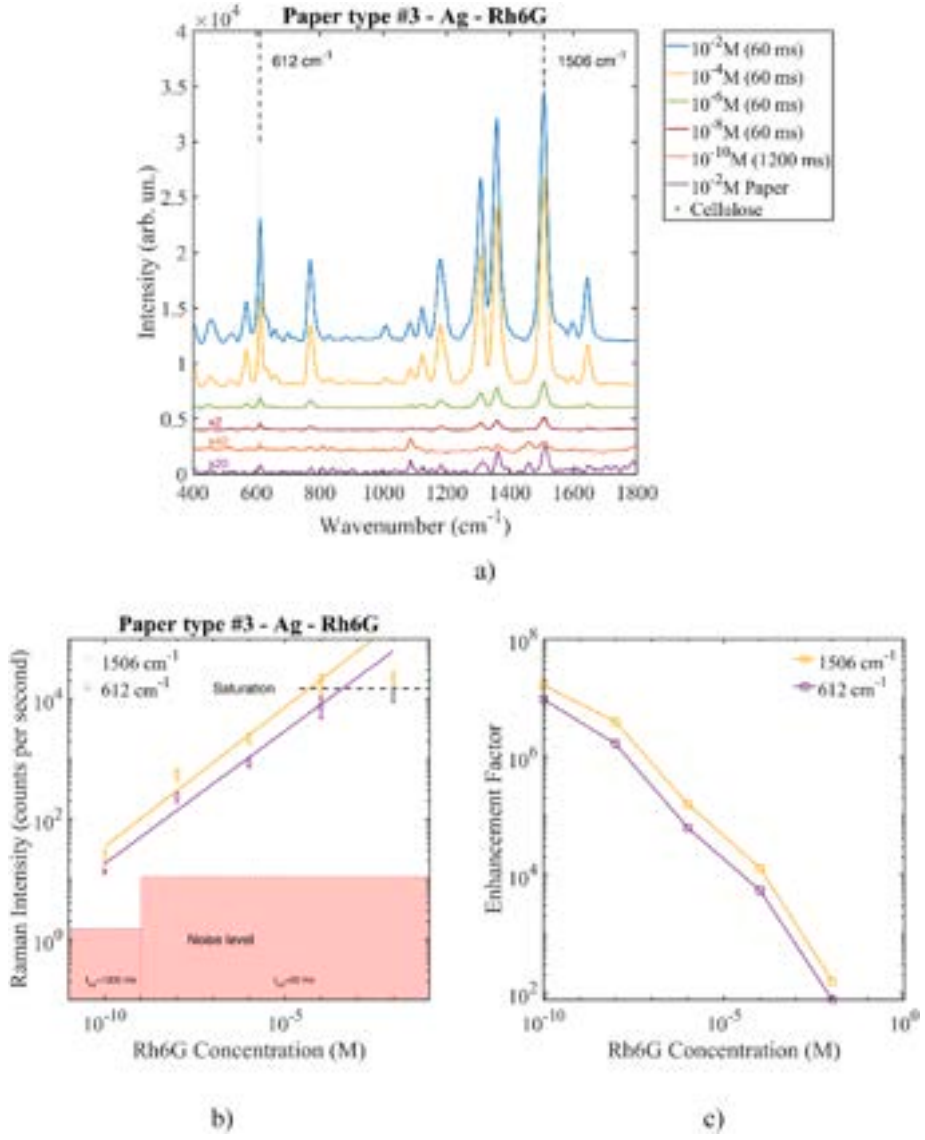

Fig. 10. paper#3: a) SERS spectra of R6G, drop-casted on sensors at concentrations ranging from 10^{-2} M to 10^{-10} M SERS; b) Raman intensity of the R6G characteristic peaks, centered at 1506 and 612 cm^{-1}; c) enhancement factor.

at 612 cm^{-1} and 1506 cm^{-1} as the concentration of Rh6G diminishes, indicating the expected decrease in signal with lower analyte levels. The calibration curves reflect a clear linear relationship between the logarithm of Rh6G concentration and the logarithm of Raman intensity, consistent across both measured peaks.

The enhancement factor reveals a downward trend with increasing Rh6G concentration.

Compared to paper#1, the results on paper#2 are very similar, indicating that the SERS substrates exhibit reproducible behavior with a slight improvement in the signal-to-noise ratio.

Fig. 10 shows SERS results for paper #3. The calibration curve still depicts a linear relationship on a log-log scale between the Raman intensity and R6G concentration, as observed for paper#1 and #2 samples. However, at the highest concentrations between 10^{-4} and 10^{-2} M, some saturation of the Raman signal is evident, diverging from linearity. This saturation suggests the limit of the substrate's enhancement capability has been reached.

Comparing the performance of the three different paper substrates all of them show a very high sensitivity that allows the detection of the test analyte at very low concentration level, down to 10^{-10} M. Apart from this important aspect, paper#1 shows a slightly lower response compared to the others across all the R6G concentrations investigated. Specifically, the intensity of the 1506 cm^{-} [1] peak (ca. 3800 cps) at the highest R6G concentration of 10^{-2} M is about 11 % (ca. 35000 cps) and 17 % (ca. 22000 cps) of the corresponding observed intensities for paper#2 and paper#3 respectively. This result is not surprising if the morphological properties of paper#1 sample are considered. As it was outlined in the discussion of the SEM images of paper#1 showed a lower density of cellulose fiber per unit area and a less dense texture with respect to the other paper samples, a feature that leads to a lower density of SERS active sites in the laser spot area, moreover the large fluctuations of the surface due to the embossed grid pattern (see Fig. 3a) can reduce the active detection area being a portion of the surface out of the detection system focal plane. Regarding the saturation observed at the highest R6G concentration of 10^{-2} M in the sample paper#3, we believe that the texture of the sample also plays a role. This sample, in fact, showed a structure like paper#2 but with a less structured array of cellulose fibers. Absorption and diffusion of the liquid through the cellulose network can play a role too due to the observed different sample textures, even if such mechanisms are hardly evaluable and out the scope of this work.

Concerning the reproducibility and uniformity of the SERS signal

acquisition of different areas were performed: in detail, a set of 5 measures have been performed for each R6G concentrations. The good standard deviation values obtained and reported in the corresponding figures, confirm the reliability and robustness of the fabrication process, ensuring consistent performance for practical applications comparable to the performance of commercial SERS sensors [54].

4. Conclusions

In this study, we successfully developed an innovative process for producing flexible SERS-active sensors using recycled paper substrates decorated with Ag nanoparticles. This involved the combination of sustainable materials and advanced characterization techniques, such as SEM, UV–Vis, and Raman spectroscopy, to evaluate the morphological, optical, and enhancement properties of the sensors.

Key findings include:

- Recycled paper substrates offer a sustainable and adaptable platform for the fabrication of SERS sensors, contributing to reduced environmental impact.
- The sensors exhibited excellent sensitivity, achieving a detection limit of 10^{-10} M for Rhodamine 6G, making them highly suitable for applications in environmental monitoring, diagnostics, and Cultural Heritage analysis.
- The recyclable nature of these SERS sensors is aligned with the concept of circular economy, allowing for continuous material reuse while minimizing waste.
- Pulsed laser deposition (PLD) of Ag nanoparticles was applied to biomass-derived substrates for the first time, yielding uniform particles distribution and high SERS activity, key factors for sensor performance.

This work underscores the importance of integrating sustainability into sensor development and highlights the potential for these eco-friendly materials to advance non-invasive detection methods. Future research should focus on further optimizing sensor performance and exploring broader applications.

CRediT authorship contribution statement

D. Giuffrida: Writing – review & editing, Writing – original draft, Visualization, Validation, Supervision, Resources, Methodology, Investigation, Formal analysis, Data curation, Conceptualization. **D. Spadaro:** Writing – review & editing, Writing – original draft, Visualization, Validation, Supervision, Resources, Methodology, Investigation, Formal analysis, Data curation, Conceptualization. **V. Strano:** Investigation, Data curation. **S. Trusso:** Writing – review & editing, Writing – original draft, Visualization, Validation, Supervision, Resources, Methodology, Investigation, Formal analysis, Data curation, Conceptualization. **M.L. Saladino:** Writing – original draft, Investigation, Formal analysis. **F. Armetta:** Writing – original draft, Investigation, Formal analysis. **R.C. Ponterio:** Writing – review & editing, Writing – original draft, Visualization, Validation, Supervision, Resources, Project administration, Methodology, Investigation, Formal analysis, Data curation, Conceptualization.

Declaration of competing interest

The authors declare that they have no known competing financial interests or personal relationships that could have appeared to influence the work reported in this paper.

Acknowledgements

We thank European Union (NextGeneration EU), through the MUR-PNRR project SAMOTHRACE — Sicilian Micro and Nano Technology Research and Innovation Center (ECS00000022); PRIN Project 2022 n. 202293AX2L "Assessment of nano/microplastics impacts – PLASTACS"; FOE 2022 project FutuRaw - The raw materials of the future from non-critical, residual and renewable sources.

The authors would like to express their gratitude to the technical staff of the mechanical workshop at CNR-IPCF Messina, D. Arigò, R. Caruso, G. Lupò, G. Sarullo, and G. Spinella, for their valuable support.

Data availability

Data will be made available on request.

References

[1] https://eur-lex.europa.eu/legal-content/EN/TXT/?qid=1583933814386&uri=COM:2020:98:FIN.
[2] https://commission.europa.eu/strategy-and-policy/priorities-2019-2024/european-green-deal_en.
[3] Z.U. Arif, M.Y. Khalid, M.F. Sheikh, A. Zolfagharian, M. Bodaghi, Biopolymeric sustainable materials and their emerging applications, J. Environ. Chem. Eng. 10 (4) (2022) 108159, https://doi.org/10.1016/j.jece.2022.108159.
[4] P. Nechita, Use of recycled cellulose fibers to obtain sustainable products for bioeconomy applications, in: Generation, Development and Modifications of Natural Fibers, IntechOpen, 2020, https://doi.org/10.5772/intechopen.86092.
[5] B.A. Helms, Polydiketoenamines for a circular plastics economy, Acc. Chem. Res. 55 (19) (2022) 2753–2765, https://doi.org/10.1021/acs.accounts.2c00308.
[6] E.A.R. Zuiderveen, K.J.J. Kuipers, C. Caldeira, S.V.K. Hanssen, M.M. van der Hulst, R. de Jonge, A. Vlysidis, R. van Zelm, S. Sala, M.A.J. Huijbregts, The potential of emerging bio-based products to reduce environmental impacts, Nat. Commun. 14 (2023) 8521, https://doi.org/10.1038/s41467-023-43797-9.
[7] A. Fiorati, A. Bellingeri, C. Punta, I. Corsi, I. Venditti, Silver nanoparticles for water pollution monitoring and treatments: ecosafety challenge and cellulose-based hybrids solution, Polymers 12 (2020) 1635, https://doi.org/10.3390/polym12081635.
[8] M.I. Bolanca, I. Majnaric, Z. Bolanca, Ecological sustainability and waste paper recycling, Procedia Eng. 100 (2015) 177–186, https://doi.org/10.1016/j.proeng.2015.01.356.
[9] H. Abushammala, M.A. Masood, S.T. Ghulam, J. Mao, On the conversion of paper waste and rejects into high-value materials and energy, Sustainability 15 (2023) 6915, https://doi.org/10.3390/su15086915.
[10] A. Claro, M.J. Melo, J. Seixas de Melo, K.J. van den Berg, A. Burnstock, M. Montague, R. Newman, Identification of red colorants in van Gogh paintings and ancient andean textiles by microspectrofluorimetry, J. Cult. Herit. 11 (1) (2010) 27–34, https://doi.org/10.1016/j.culher.2009.03.006.
[11] C. Clementi, C. Miliani, A. Romani, U. Santamaria, F. Morresi, K. Mlynarska, G. Favaro, In-situ fluorimetry: a powerful non-invasive diagnostic technique for natural dyes used in artefacts, Spectrochim. Acta Mol. Biomol. Spectrosc. 71 (5) (2009) 2057–2062, https://doi.org/10.1016/j.saa.2008.08.006.
[12] M.C. Caggiani, P. Colomban, Advanced procedures in Raman forensic, natural, and cultural heritage studies: mobile set-up, optics, and data treatment—state of the art and perspectives, J. Raman Spectrosc. 55 (2) (2024) 116, https://doi.org/10.1002/jrs.6633.
[13] S. Innocenti, D. Quintero Balbas, M. Galeotti, A. Cagnini, S. Porcinai, J. Striova, Historical pigments and paint layers: Raman spectral library with 852 nm excitation laser, Minerals 14 (2024) 557, https://doi.org/10.3390/min14060557.
[14] J. Romero-Pastor, A. Duran, A.B. Rodríguez-Navarro, R. van Grieken, C. Cardell, Compositional and quantitative microtextural characterization of historic paintings by micro-X-ray diffraction and Raman microscopy, Anal. Chem. 83 (2011) 8420–8428.
[15] F. Casadio, M. Leona, J.R. Lombardi, R. Van Duyne, Identification of organic colorants in fibers, paints and glazes by surface enhanced Raman spectroscopy, Acc. Chem. Res. 43 (6) (2010) 782–791, https://doi.org/10.1021/ar100019q.
[16] X.X. Han, R.S. Rodriguez, C.L. Haynes, Y. Ozaki, B. Zhao, Surface-enhanced Raman spectroscopy, Nat. Rev. Methods Primers 1 (2021) 87, https://doi.org/10.1038/s43586-021-00083-6.
[17] V. Mollica Nardo, V. Renda, S. Trusso, R.C. Ponterio, Role of pH on nanostructured SERS active substrates for detection of organic dyes, Molecules 26 (2021) 2360, https://doi.org/10.3390/molecules26082360.
[18] V. Mollica Nardo, A. Sinopoli, L. Kabalan, R.C. Ponterio, F. Saija, S. Trusso, SERS and DFT study of indigo adsorbed on silver nanostructured surface, Spectrochim. Acta Mol. Biomol. Spectrosc. 205 (2018) 465–469, https://doi.org/10.1016/j.saa.2018.07.059.
[19] E. Fazio, S. Trusso, R.C. Ponterio, Surface-enhanced Raman scattering study of organic pigments using silver and gold nanoparticles prepared by pulsed laser ablation, Appl. Surf. Sci. 272 (2013) 36–41, https://doi.org/10.1016/j.apsusc.2012.02.070.
[20] S. Trusso, G. Festa, C. Scatigno, G. Romanelli, A. Piperno, R.C. Ponterio, Neutron sensing at spallation neutron sources by SERS, Appl. Surf. Sci. 651 (2024) 159186, https://doi.org/10.1016/j.apsusc.2023.159186.
[21] N.R. Agarwal, M. Tommasini, E. Fazio, S. Trusso, R.C. Ponterio, SERS activity of silver and gold nanostructured thin films deposited by pulsed laser ablation, Appl. Phys. A 117 (2014) 347–351, https://doi.org/10.1007/s00339-014-8401-8.

[22] A. Camposeo, D. Spadaro, D. Magrì, M. Moffa, P. Gucciardi, L. Persano, O. M. Maragò, D. Pisignano, Surface-enhanced Raman spectroscopy in 3D electrospun nanofiber mats coated with gold nanorods, Anal. Bioanal. Chem. 408 (2016) 1357–1364, https://doi.org/10.1007/s00216-015-9226-9.
[23] Z. Yao, P. Coatsworth, X. Shi, J. Zhi, L. Hu, R. Yan, F. Güder, H.D. Yu, Paper-based sensors for diagnostics, human activity monitoring, food safety and environmental detection, Sens. Diagn 1 (2022) 312, https://doi.org/10.1039/d2sd00017b.
[24] A.T. Singh, D. Lantigua, A. Meka, S. Taking, P. Manjot, G. Camci-Unal, Paper-based sensors: emerging themes and applications, Sensors 18 (2018) 2838, https://doi.org/10.3390/s18092838.
[25] A. Fularz, S. Almohammed, J.H. Rice, SERS enhancement of porphyrin-type molecules on metal-free cellulose-based substrates, ACS Sustain. Chem. Eng. 9 (49) (2021) 16808–16819, https://doi.org/10.1021/acssuschemeng.1c06685.
[26] M. Herrero, Towards green extraction of bioactive natural compounds, Anal. Bioanal. Chem. 416 (2024) 2039–2047, https://doi.org/10.1007/s00216-023-04969-0.
[27] Y. Fang, N.H. Seong, D.D. Dlott, Measurement of the distribution of site enhancements in surface-enhanced Raman scattering, Science 321 (5887) (2008) 388–392, https://doi.org/10.1126/science.1159499.
[28] S.A. Ogundare, W.E.A. van Zyl, Review of cellulose-based substrates for SERS: fundamentals, design principles, applications, Cellulose 26, fasc. 11 (luglio 2019) 6489–6528, https://doi.org/10.1007/s10570-019-02580-0.
[29] Y. Lu, L. Yan L. Zehao, H. Jianguo, A silver-nanoparticle/cellulose-nanofiber composite as a highly effective substrate for surface-enhanced Raman spectroscopy, Beilstein J. Nanotechnol. (2019), https://doi.org/10.3762/BJNANO.10.126.
[30] M. Ammara, H. Shafqat, N. Al-A. Ameenah, A.-A. Abdel-Haleem, Ur R. Zia, Hamza Qayyum, Laser-based synthesis of silver nanoparticles embedded in cellulose paper for catalytic reduction of azo dyes and SERS sensing of pesticides, Phys. Scripta 99 (2024) 075940, https://doi.org/10.1088/1402-4896/ad5230.
[31] H.-Y. Lin, W.-R. Chen, L.-C. Lu, H.-L. Chen, Y.-H. Chen, M. Pan, C. Chen, C. Chen, T.-H. Yen, D. Wan, Direct thermal growth of gold nanopearls on 3D interweaved hydrophobic fibers as ultrasensitive portable SERS substrates for clinical applications, Small 19 (2023) 2207404, https://doi.org/10.1002/smll.202207404.
[32] M. Verma, T.K. Naqvi, K.T. Santosh, M.K. Manish, K.D. Prabhat, Paper based low-cost flexible SERS sensor for food adulterant detection, Environ. Technol. Innovat. 24 (2021) 102033, https://doi.org/10.1016/j.eti.2021.102033.
[33] L.L. Tay, S. Poirier, A. Ghaemi, J. Hulse, Inkjet-printed paper-based surface enhanced Raman scattering (SERS) sensors for the detection of narcotics, MRS Adv. 7 (2022) 190–196, https://doi.org/10.1557/s43580-022-00257-8.
[34] W.W. Yu, I.M. White, Inkjet printed surface enhanced Raman spectroscopy array on cellulose paper, Anal. Chem. 82 (23) (2010) 9626–9630, https://doi.org/10.1021/ac102475k.
[35] L. Xie, H. Zeng, J. Zhu, Z. Zhang, H. Sun, W. Xia, Y. Du, State of the art in flexible SERS sensors towards label-free and on-site detection: from design to applications, Nano Res. 15 (5) (2022) 4374–4394, https://doi.org/10.1007/s12274-021-4017-4.
[36] S. Roh, T. Chung, B. Lee, Overview of the characteristics of micro- and nano-structured surface plasmon resonance sensors, Sensors 11 (2011) 1565–1588, https://doi.org/10.3390/s110201565.
[37] S. Verma, B.T. Rao, S. Rai, V. Ganesan, L.M. Kukreja, Influence of process parameters on surface plasmon resonance characteristics of densely packed gold nanoparticle films grown by pulsed laser deposition, Appl. Surf. Sci. 258 (11) (2012) 4898–4905, https://doi.org/10.1016/j.apsusc.2012.01.111.
[38] E. Fazio, F. Neri, R.C. Ponterio, S. Trusso, M. Tommasini, P.M. Ossi, Laser controlled synthesis of noble metal nanoparticle arrays for low concentration molecule recognition, Micromachines 5 (2014) 1296–1309, https://doi.org/10.3390/mi5041296.
[39] C. D'Andrea, F. Neri, P.M. Ossi, N. Santo, S. Trusso, The controlled pulsed laser deposition of Ag nanoparticle arrays for surface enhanced Raman scattering, Nanotechnology 20 (2009) 245606, https://doi.org/10.1088/0957-4484/20/24/245606.
[40] E. Fazio, F. Neri, C.D. Andrea, P.M. Ossi, N. Santo, S. Trusso, SERS activity of pulsed laser ablated silver thin films with controlled nanostructure, J. Raman Spectrosc. 42 (2011) 1298, https://doi.org/10.1002/jrs.2861.
[41] F. Neri, P.M. Ossi, S. Trusso, Cluster synthesis and assembling in laser-generated plasmas, Riv. Nuovo Cimento 34 (2011) 103–149.
[42] C. Zhan, X.-J. Chen, J.Yi Li, D.-Y. Wu, Z.-Q. Tian, From plasmon-enhanced molecular spectroscopy to plasmon-mediated chemical reactions, Nat. Rev. Chem 2 (2018) 216–230, https://doi.org/10.1038/s41570-018-0031-9.
[43] E. Hutter, J.H. Fendler, Exploitation of localized surface plasmon resonance, Adv. Mater. 16 (19) (2004) 1685–1706, https://doi.org/10.1002/adma.200400271.
[44] K.A. Willets, R.P. Van Duyne, Localized surface plasmon resonance spectroscopy and sensing, Annu. Rev. Phys. Chem. 58 (2007) 267–297, https://doi.org/10.1146/annurev.physchem.58.032806.104607.
[45] B. Fazio, S. Trusso, E. Fazio, F. Neri, P.M. Ossi, N. Santo, Nanostructured silver thin films deposited by pulsed laser ablation, Radiat. Eff. Defect Solid 163 (2008) 673–683, https://doi.org/10.1080/10420150701781001.
[46] N.R. Agarwal, E. Fazio, F. Neri, S. Trusso, C. Castiglioni, A. Lucotti, N. Santo, P. M. Ossi, Ag and Au nanoparticles for SERS substrates produced by pulsed laser ablation, Cryst. Res. Technol. 46 (2011) 836–840, https://doi.org/10.1002/crat.201000588.
[47] N.R. Agarwal, P.M. Ossi, S. Trusso, Driving electromagnetic field enhancements in tailored gold surface nanostructures: optical properties and macroscale simulations, Appl. Surf. Sci. 466 (2019) 19–27, https://doi.org/10.1016/j.apsusc.2018.09.251. ISSN 0169-4332.
[48] C. Zanchi, A. Lucotti, M. Tommasini, M. Pistaffa, L. Giuliani, S. Trusso, P.M. Ossi, Pulsed laser deposition of gold thin films with long-range spatial uniform SERS activity, Appl. Phys. A 125 (2019) 311, https://doi.org/10.1007/s00339-019-2527-7.
[49] Miniconoscan launch a compact, cost-efficient system for high accuracy 3D scanning, Sens. Rev. 21 (3) (2001), https://doi.org/10.1108/sr.2001.08721cad.013.
[50] S. Roh, T. Chung, B. Lee, Overview of the characteristics of micro- and nano-structured surface plasmon resonance sensors, Sensors 11 (2011) 1565–1588, https://doi.org/10.3390/s110201565.
[51] S. Verma, B.T. Rao, S. Rai, V. Ganesan, L.M. Kukreja, Influence of process parameters on surface plasmon resonance characteristics of densely packed gold nanoparticle films grown by pulsed laser deposition, Appl. Surf. Sci. 258 (2012) 4898–4905, https://doi.org/10.1016/j.apsusc.2012.01.111.
[52] X.N. He, Y. Gao, M.M. Samani, P.N. Black, J. Allen, M. Mitchell, W. Xiong, Y. S. Zhou, L. Jiang, Y.F. Lu, Surface-enhanced Raman spectroscopy using gold-coated horizontally aligned carbon nanotubes, Nanotechnology 23 (2012) 205702, https://doi.org/10.1088/0957-4484/23/20/205702.
[53] P.A. Mercadal, E.R. Encina, J.E.L. Villa, E.A. Coronado, A new figure of merit to assess the SERS enhancement factor of colloidal gold nanoparticle aggregates, J. Phys. Chem. C 125 (2021) 4056–4065, https://doi.org/10.1021/acs.jpcc.0c09122.
[54] M. Rahmani, P. Taugeron, A. Rousseau, N. Delorme, L. Douillard, L. Duponchel, J.-F. Bardeau, Highlight on commercial SERS substrates and on optimized nanorough large-area SERS-based sensors: a Raman study, Appl. Nanosci. 14 (2024) 203–215, https://doi.org/10.1007/s13204-023-02972-6.